MAD Observations of the galactic star clusters HP1 and FSR 1415

S. Ortolani

and

Y. Momany, B. Barbuy, E. Bica, C. Bonatto

- Search for new low latitude old star cluster candidates in the direction of the galactic bulge
- Detailed study of confirmed candidates
- New discoveries 2006-2008:
- AL3: l=3.4, b=-5.3, D=6.0, [Fe/H]=-1.3 (bulge)
- FSR584: l=184, b=0.84, D=1.4, [Fe/H]=-2.0
- FSR1767: l=352, b=-2.2, D=1.5, [Fe/H]=-1.2
- ESO 92-SC05: l = 286, b=-7, D=10.9

- **A new interesting old star cluster: FSR 1415 (l=263, b=-1.8), good for MAD**

The problem of field contamination

- 2 basic techniques:
- 1) central extraction and statistical decontamination using a nearby field
- 2) proper motion cleaning (+ radial velocities ?)

(1) Requires high resolution and uniform star background distribution (uniform reddening). It works well at relatively high latitudes

(2) Requires high astrometric accuracy and two epochs. It works well when there is a high tangential motion reltively to the field. This condition is usully verified with clusters having a low radial velocity (typically lower than 80-90 km/s)

Mon. Not. R. Astron. Soc. 391, 1650–1658 (2008) doi:10.1111/j.1365-2966.2008.

Multi-Conjugate Adaptive Optics VLT imaging of the distant old open cluster FSR 1415

Y. Momany,[1,2★] S. Ortolani,[3] C. Bonatto,[4] E. Bica[4] and B. Barbuy[5]

[1]INAF, Osservatorio Astronomico di Padova, Vicolo dell'Osservatorio 5, I-35122 Padova, Italy
[2]European Southern Observatory, Alonso de Cordova 3107, Santiago, Chile
[3]Università di Padova, Dipartimento di Astronomia, Vicolo dell'Osservatorio 2, I-35122 Padova, Italy
[4]Universidade Federal do Rio Grande do Sul, Departamento de Astronomia CP 15051, RS, Porto Alegre 91501-970, Brazil
[5]Universidade de São Paulo, IAG, Rua do Matão 1226, Cidade Universitária, São Paulo 05508-900, Brazil

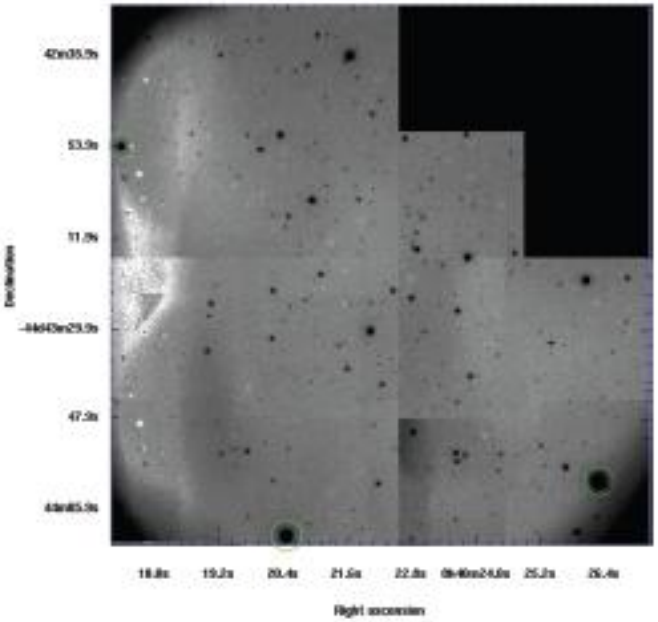

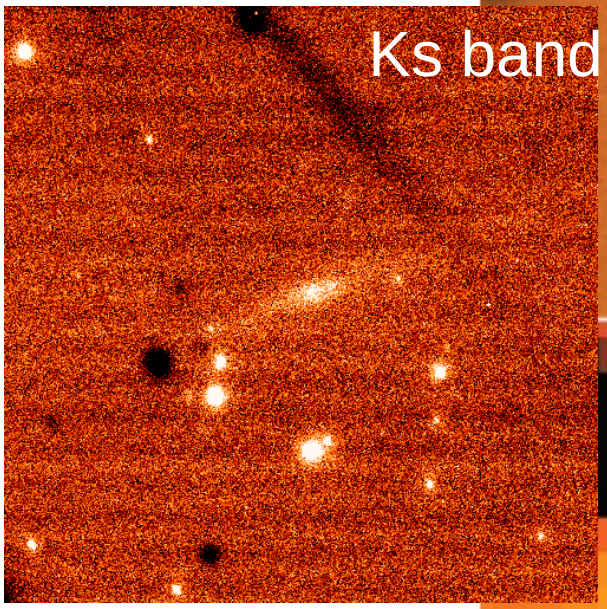

Figure 1. The MAD mosaic of the eight *J*- and *k*-dithered images of FSR 1415: east is to the right and north to the top. The overall circular field of view is ~1.8 × 1.8 arcmin. The irregular shape of the mosaic is due to the lacking of a fifth dithered image. Border vignetting and other features (due to the movable scanning table) are unavoidable.

FoV: 3.25 arcmin

FWHM: 75 mas (K), 140 mas (J)

t: 1080 s (J,K)

DIMM: 0”.8

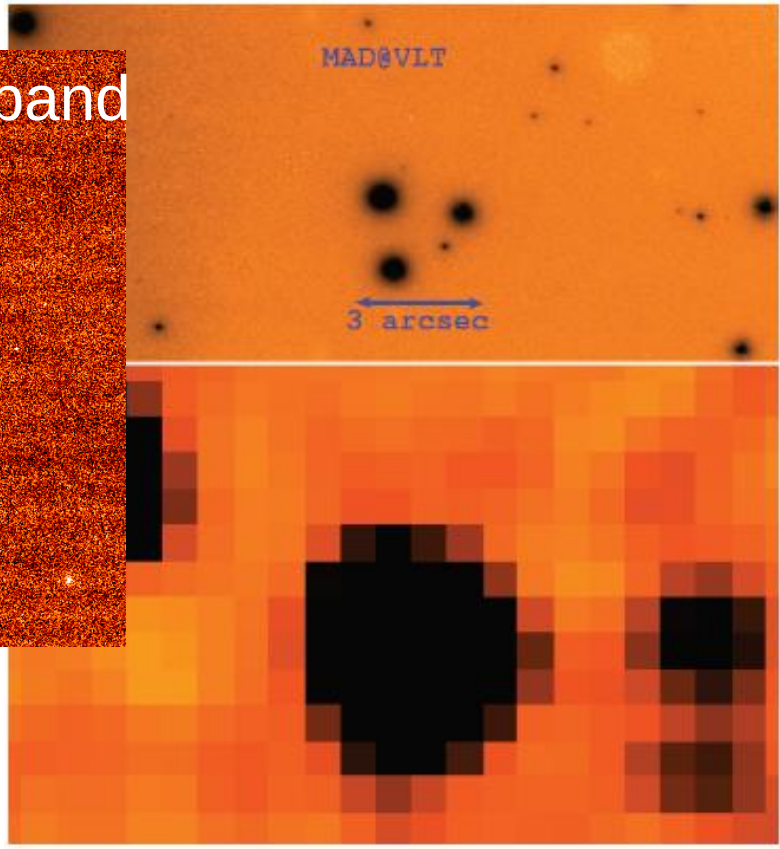

Figure 3. The resolution supremacy of the MAD *K* image as compared to the 2MASS. The quadruple MAD stars with *K* magnitudes of 13.536, 13.868, 14.391 and 17.155 are identified as one single star ($K = 12.853 \pm 0.040$ and $J = 13.536 \pm 0.038$) in the 2MASS catalogue.

FSR 1415
MAD + 2MASS

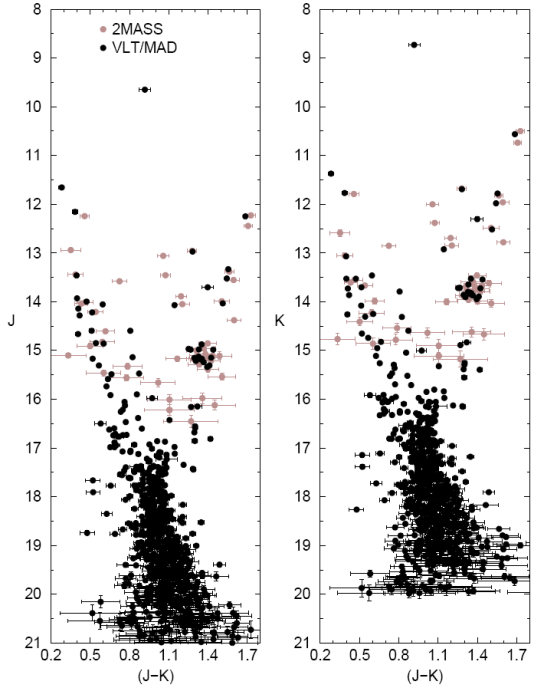

models subtr.

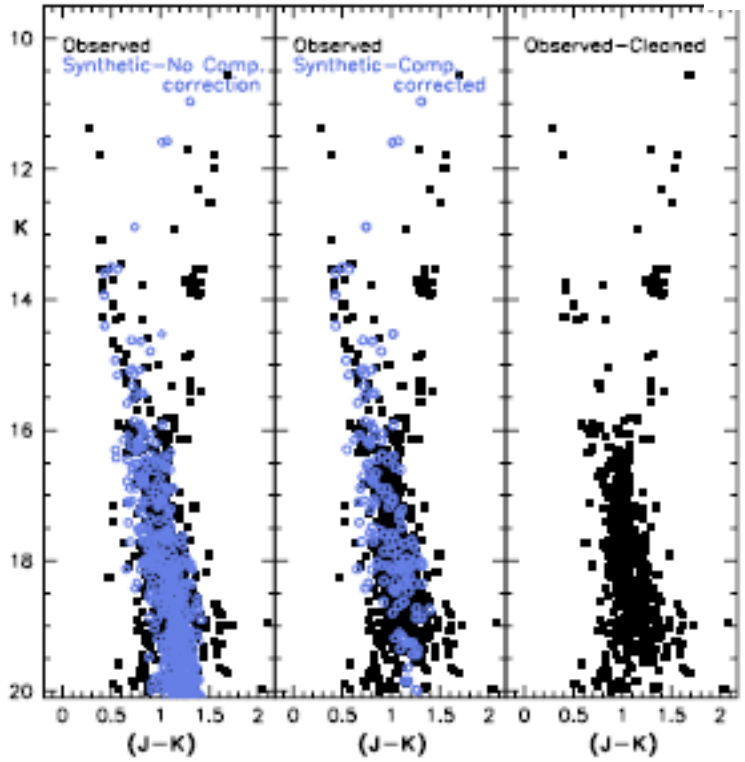

sky subtr. (open loop)

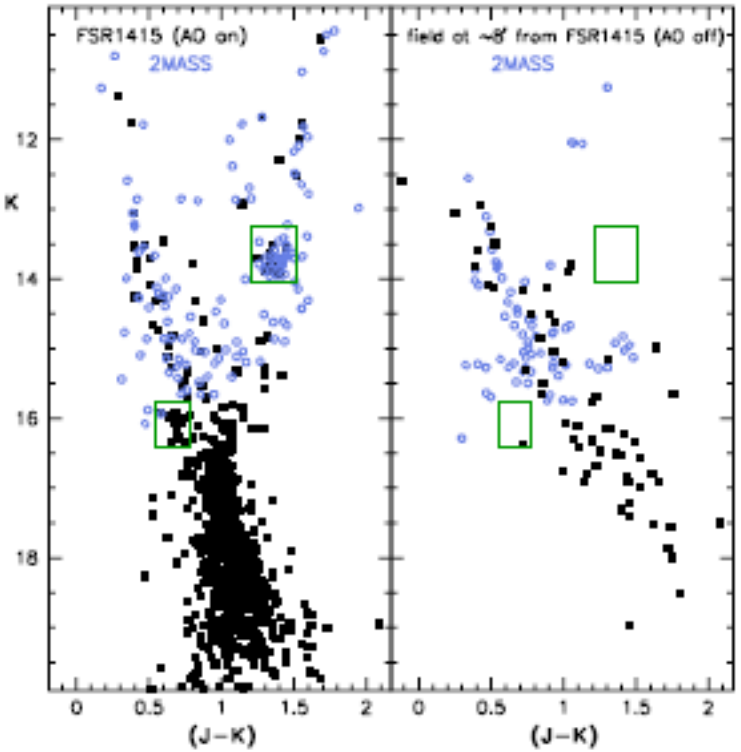

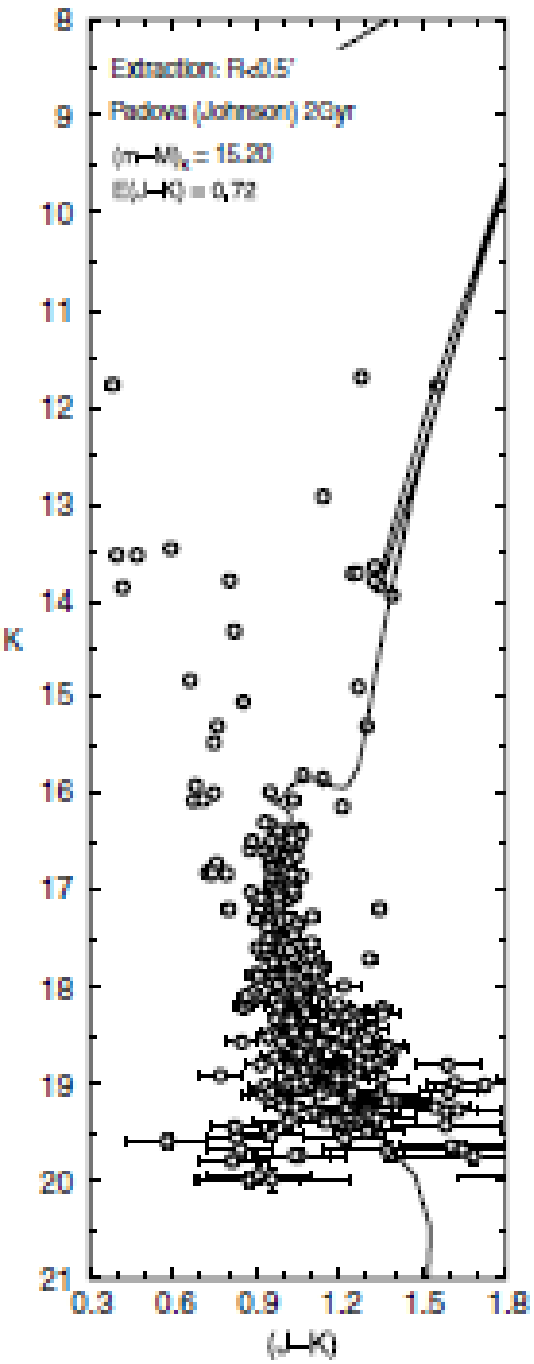

- t = 2.5 Gyr
- Z = 0.02
- D = 7.2 Kpcs
- Old open cluster confirmed

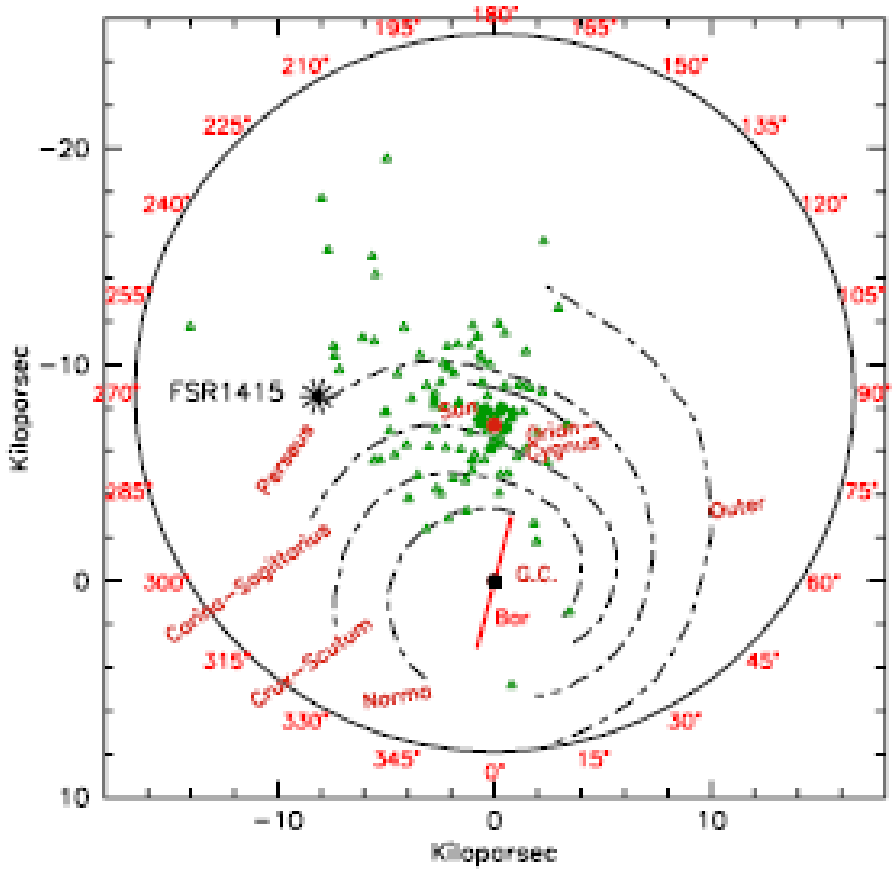

Figure 10. A schematic view of the Milky Way as seen from its North Pole showing the four spiral arms, the Galactic Centre and the Sun's position (with $R_{\odot} = 7.2 \pm 0.3$ kpc). Also plotted are a WEBDA open cluster compilation (limited to an age of $\geq$1 Gyr) and the position of FSR 1415 as derived in this paper.

Second MAD science demonstration period: globular clusters in the galactic bulge

The Proper Motion of the Globular Cluster NGC 6553 and of Bulge Stars with HST

M. Zoccali, A. Renzini, S. Ortolani, E. Bica, B. Barbuy (AJ, 121, 2638 2001)

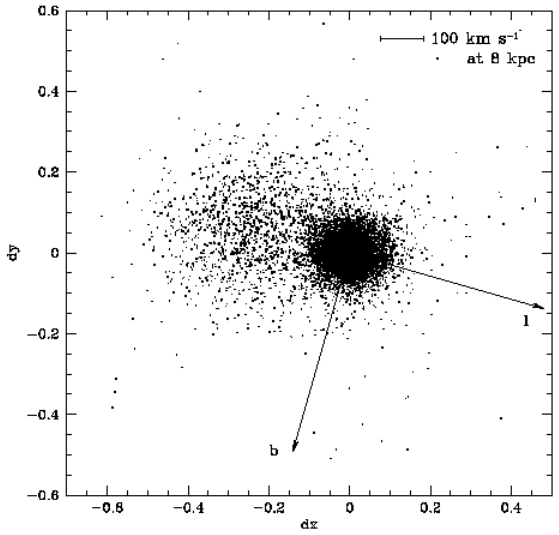

Fig. 3.— Relative proper motions (dx,dy) in pixels between the two epochs. The arrows show the direction of increasing Galactic longitude (l) and latitude (b).

Vr=3-6 km/s

About 6 mas/year, corr. to

100 km/s at 8 Kpcs

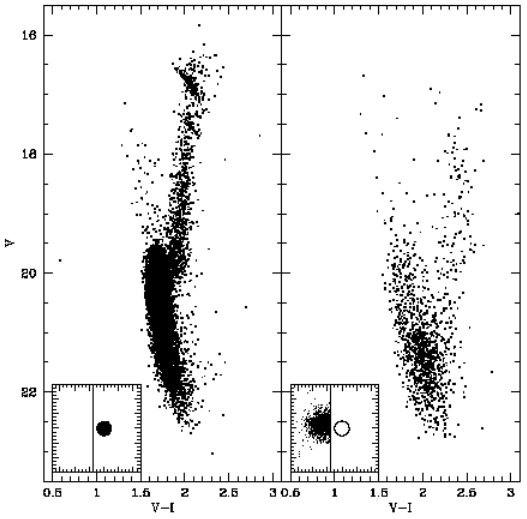

Fig. 4.— Left panel: NGC 6553 stars, selected as those lying inside a radius of 0.1 pixels centered on (0,0) in Fig. 3 (reproduced in the panel inset). We selected the stars inside a relatively small radius in order to obtain the cleanest possible cluster CMD. Right panel: CMD of (mainly) bulge stars, selected as those having $dx < -0.15$ in Fig. 3. Cluster stars are still present in this CMD because, being much more numerous, a still appreciable number of them fall well ouside the selected cluster circle.

MAD: the metal poor bulge globular cluster HP1

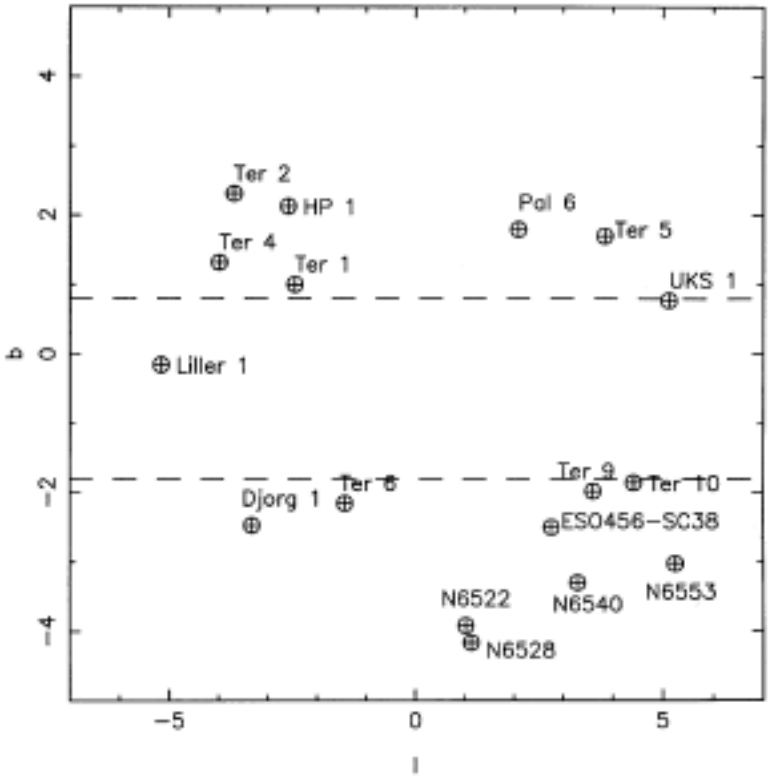

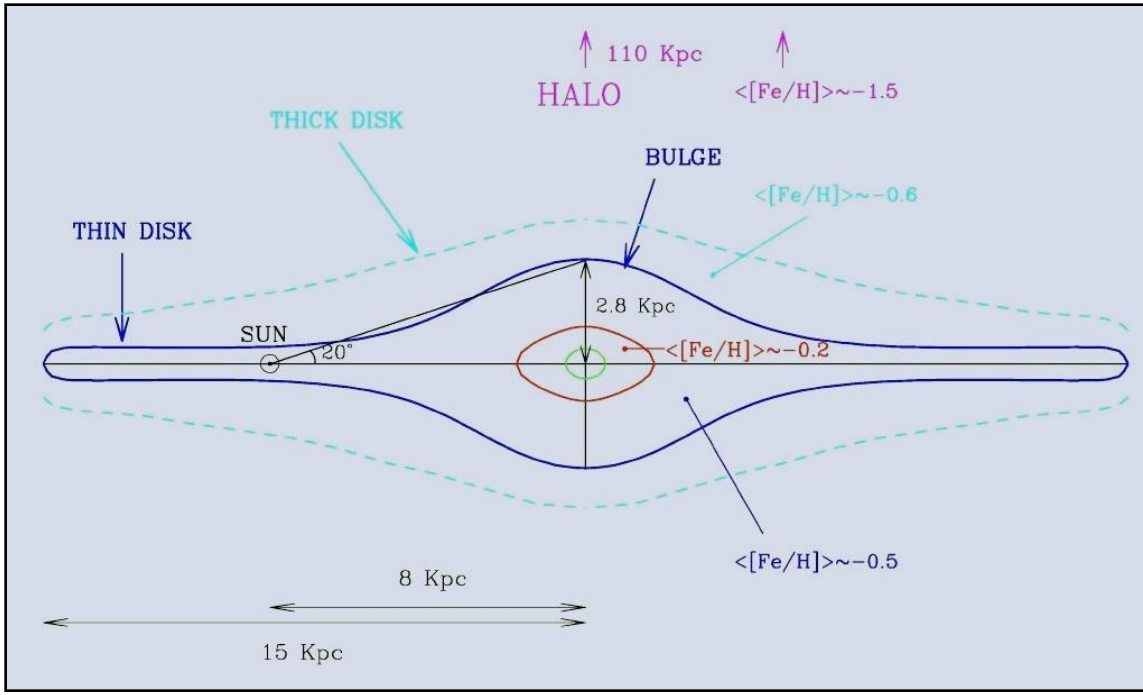

Fig. 1. Angular distribution of the sample clusters. The dashed lines represent the limit for cluster occurrence (except Liller 1).

HP1 NTT+SUSI
V=10m, I=4m, FWHM = 0.5”

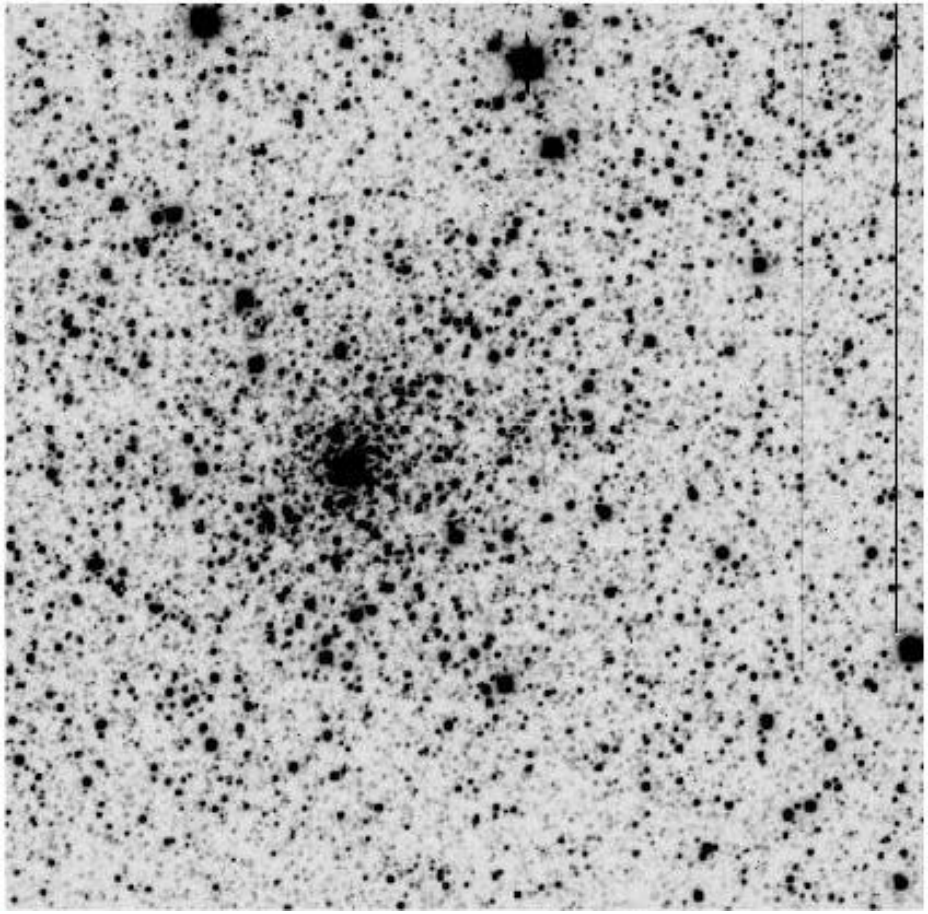

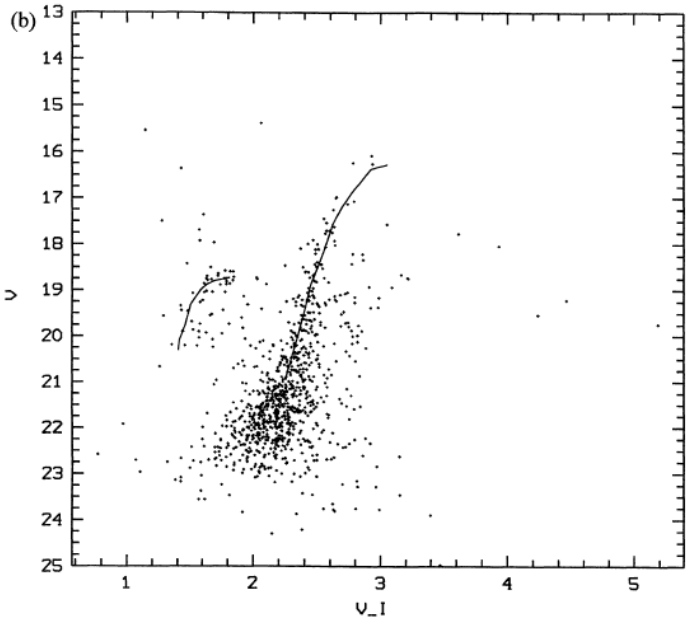

Figure 2. (a) V versus $(V-I)$ CMD for an extraction of radius $r < 23$ arcsec centred on the cluster; (b) same as (a), with the mean locus of NGC 6752 superimposed on the metal-poor sequences.

HP1: proper motion
NTT '94 vs. WFI 2002
Used for the selection of the UVES targets

Results:
[Fe/H]=-1.0, [O, Si/Fe]=0.3
Vr=56 km/s

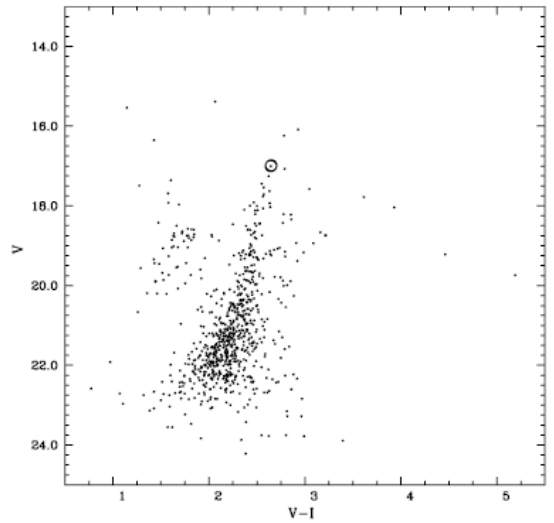

Fig. 2. The NTT-SUSI V vs. $V-I$ CMD of HP-1 with the target stars (they are almost coincident) indicated.

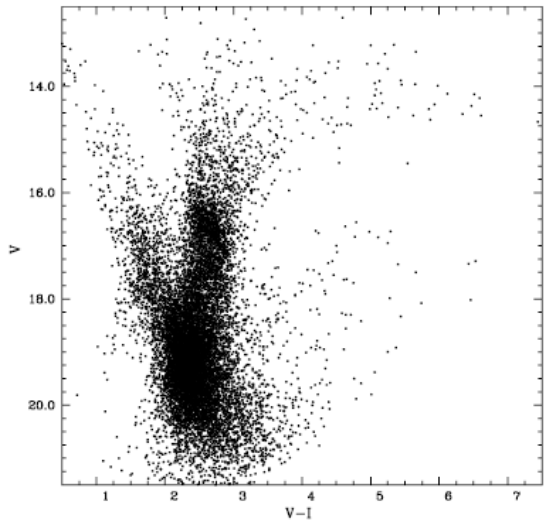

Fig. 3. The WFI V vs. $V-I$ CMD of HP-1. Size of extraction is $5' \times 5'$.

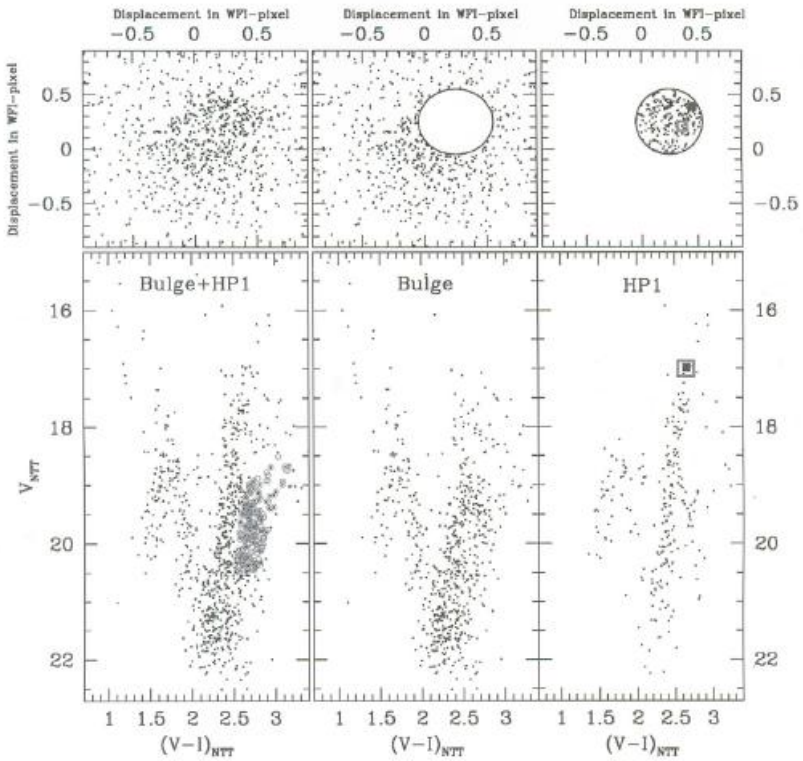

Fig. 4. The WFI and NTT data used to establish proper motion cleaning of the field.

HP1 MAD observations, some observing problems…

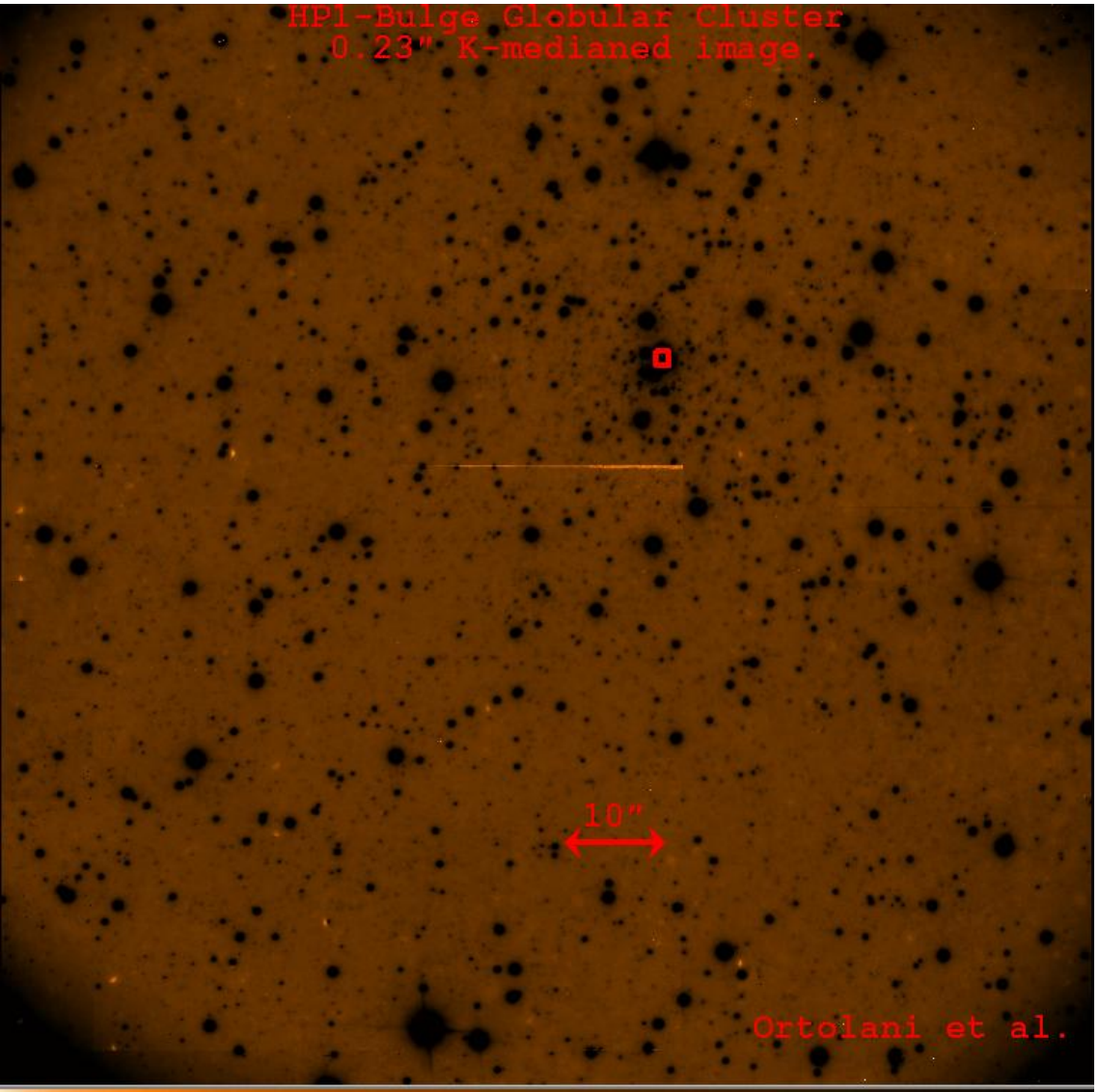

FWHM: 0.23” K, 0.37” J

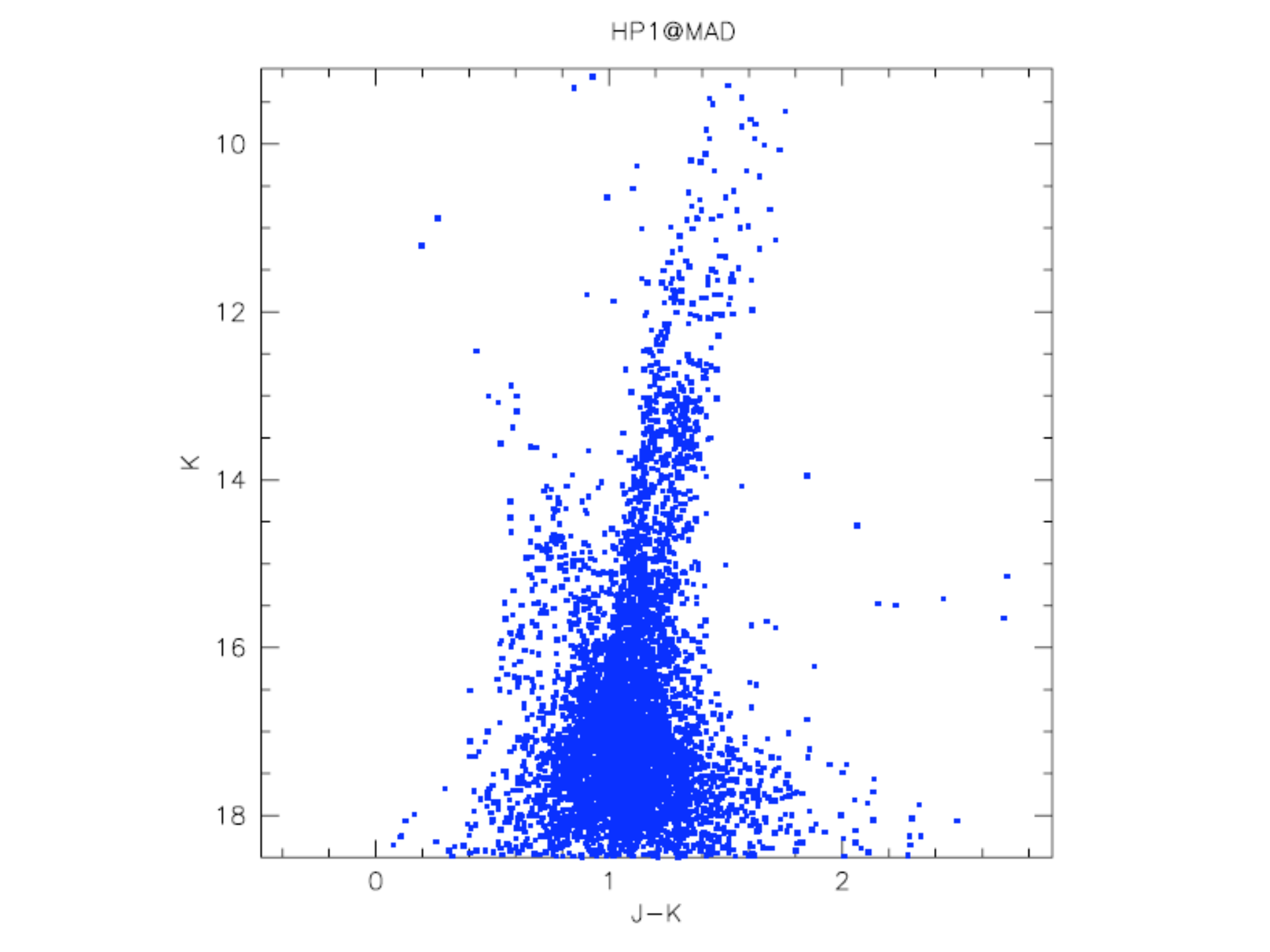
HP1@MAD
K
10
12
14
16
18
0
1
2
J−K

HP1 (Vr=60 km/s)：MAD (2008)- NTT(1994), 6 mas/year

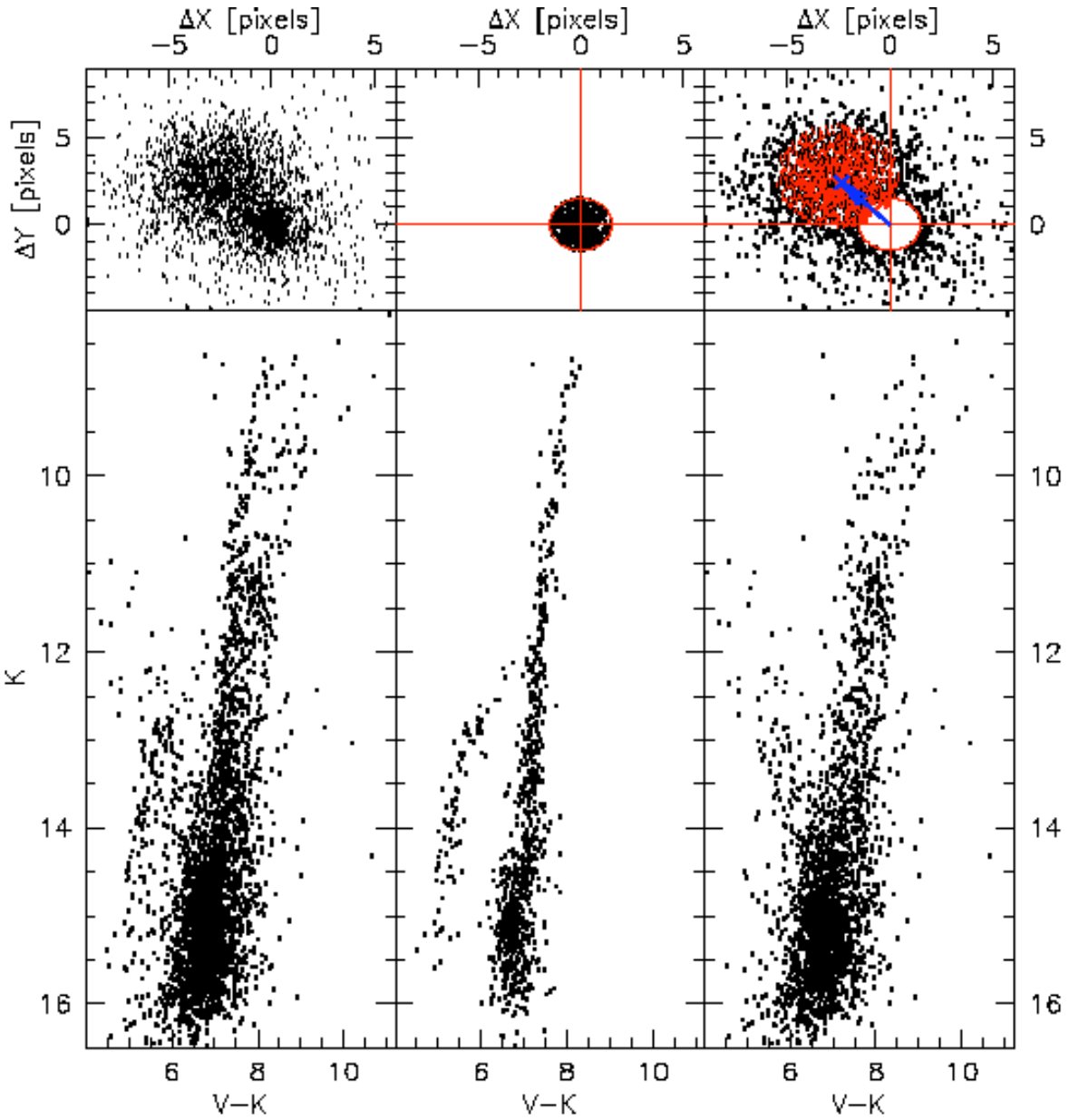

Observations of template failed

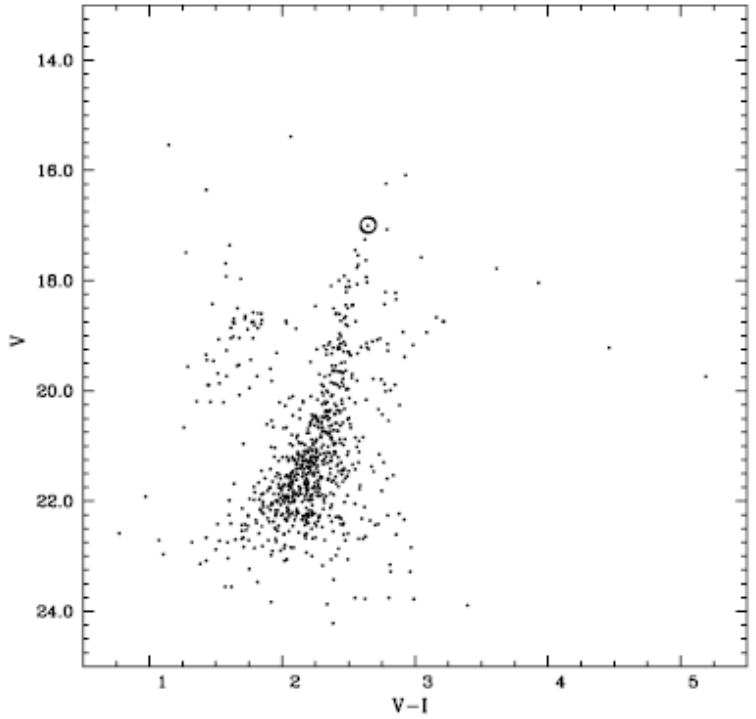

Fig. 2. The NTT-SUSI V vs. $V-I$ CMD of HP-1 with the target stars (they are almost coincident) indicated.

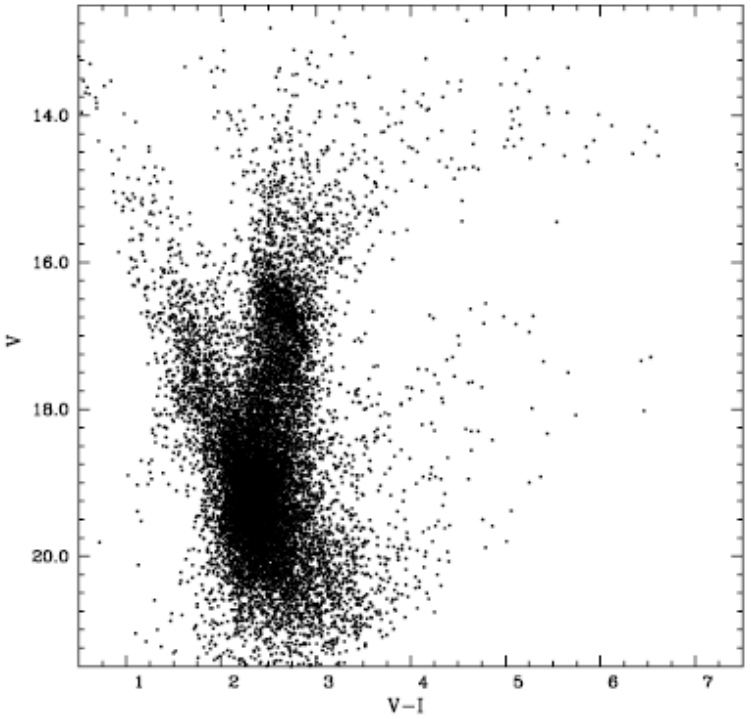

Fig. 3. The WFI V vs. $V-I$ CMD of HP-1. Size of extraction is $5' \times 5'$.

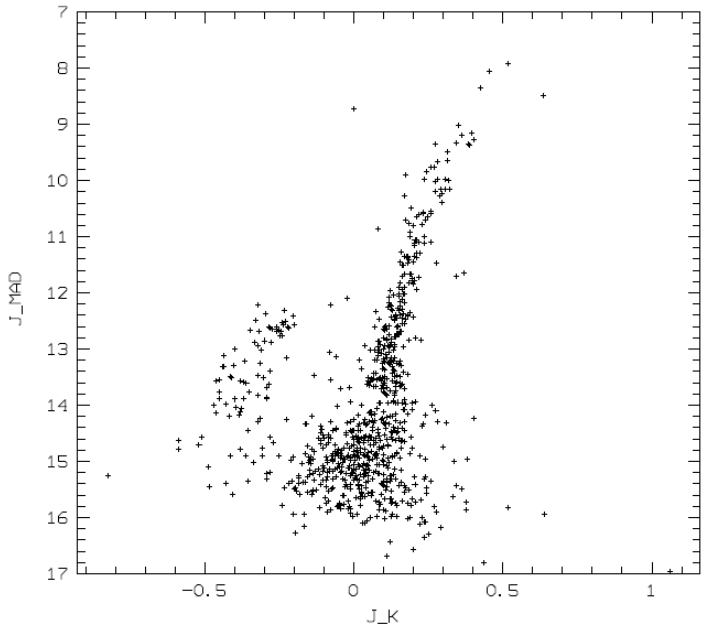

HP1 MAD/NTT plots

B-R/B+V+R=0.85

[Fe/H]=-1.0

old age

Different combinations and/or techniques can be tested (i.e. input positions)